Chemical Science

Accepted Manuscript

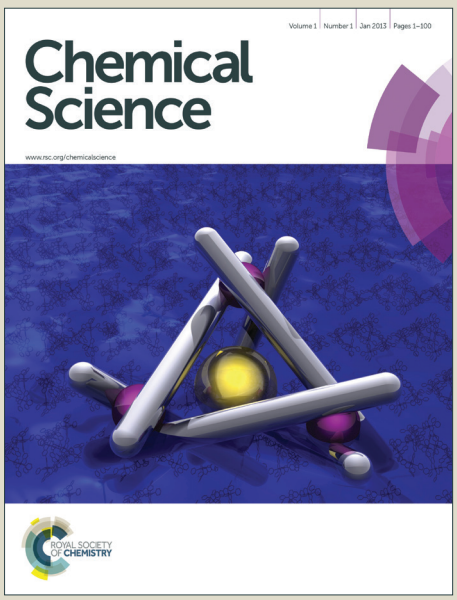

ROYAL SOCIETY OF CHEMISTRY

www.rsc.org/chemicalscience

Journal Name

RSCPublishing

ARTICLE

Dissipative Assembly of a Membrane Transport System

Cite this: DOI: 10.1039/x0xx00000x

A.K. Dambenieks,[a] P.H.Q. Vu[a] and T.M. Fyles[a],

Received 00th January 2012,
Accepted 00th January 2012

DOI: 10.1039/x0xx00000x

www.rsc.org/

A membrane system consisting of a transport-inactive thiol-terminated oligioester and a channel-forming amine-terminated thioester is subject to kinetic control though the provision of a chemical fuel. Intermolecular thioester exchange occurs rapidly between the fuel and the inactive thiol to produce the channel-forming species. Spontaneous intramolecular degradation of the active compound with release of a lactam occurs more slowly to reform the inactive thiol. The system can cycle from transport inactive to active and back via injection of the fuel. Such behavior is consistent with dissipative assembly of the ion-channel function of the system.

Living organisms exist in an open non-equilibrium state which consumes matter and energy from, and releases wastes to, the environment. At the same time cells are closed, organized, complex reaction networks that exploit energy and material fluxes to create and maintain structures and functions. Leaving aside the philosophical questions of whether these observations are among the necessary and sufficient conditions to recognize "life"[1, 2], there remain important questions about the self-assembly of structures via harnessing of energy fluxes. Sometimes called "dynamic self-assembly"[3-6], dissipative assembly of artificial systems has largely focused on the creation of mesoscopic structures whose emergence depends on continuous energy input[3, 6]. Examples include chemical oscillator reaction networks that form travelling waves[7] but which can also form stable Turing patterns in two[8] and three dimensions[9] under conditions that depend on the relative diffusion rates of reaction inhibitors and activators. In a non-chemical system, magneto-hydrodynamic interactions allow the creation of stable patterns of floating magnets in a rotating magnetic field[10]. The interaction of a ferrofluid with a hydrophobic surface allows such patterns to be switched in response to variable magnetic fields[11]. A wide range of forces and fields can potentially be exploited in the same fashion[3, 6].

In Nature, dissipative assembly occurs via the synthesis of non-assembling building blocks that are activated for assembly through chemical energy input. The assembled structure is maintained so long as there is available input energy; when the input energy is dissipated the structure disassembles to the building blocks. Such a system occurs in microtubule formation where precursor proteins (tubulins) are activated for tubule assembly via GTP phosphorylation[12]. Subsequent hydrolysis of the tubulin results in collapse of the microtubule. The assembly is therefore driven by the dissipation of the 50 kJ/mol of hydrolysis free energy available from GTP. Bioinspired materials based on tubulin demonstrate dissipative assembly in vitro[13, 14] and offer a route to mesoscale machines[15]. An abiological example is the dissipatively assembled gelator reported by van Esch and co-workers[16]. In this system the energy source is the basic hydrolysis of methyl iodide via an intermediate carboxylic acid diester, the gelator, which subsequently hydrolyses. In chemically activated systems, the rate of activation must be fast relative to the deactivation to ensure a sufficient concentration of the metastable intermediate. Such systems have the same kinetic basis as the formation of Turing structures in chemical oscillators[9].

The important outcome of dissipative assembly in Nature is not structure but *function*; the microtubule system exists to transport materials within the cell and has evolved to assemble a functional structure only when required[12]. The process is under exquisite feedback control, but the overall energetics are simple: function is associated with a metastable intermediate[16]. In many of the cases cited above, it is the structure which is detected, but this is not fundamental. As system size shrinks from the meso- to nano-scale, the detection of the *structure* of the intermediate state becomes more challenging, but that need not inhibit the exploration of the *function* of a dissipatively assembled system. All that is required is the ability to detect the action of the metastable state of the system with a functional assay; the inversion of the reaction vial served this purpose in the gelation system[16].

In a strictly biomimetic approach, the ionic gradients across bilayer membranes might be seen as an energy source, but it is more productive to view the conductivity changes associated with membrane transport as an indicator of a functional state. The voltage-clamp experiment is potentially a single-molecule detector, capable of reporting the transport function at millisecond resolution[17]. Even bulk experiments using vesicles are rapid and sensitive functional assays of the existence of a transporter within a complex mixture[18].

Figure 1: Design of a dissipative assembly of a membrane transport system. A: schematic energy profile. B: Proposed implementation of the design.

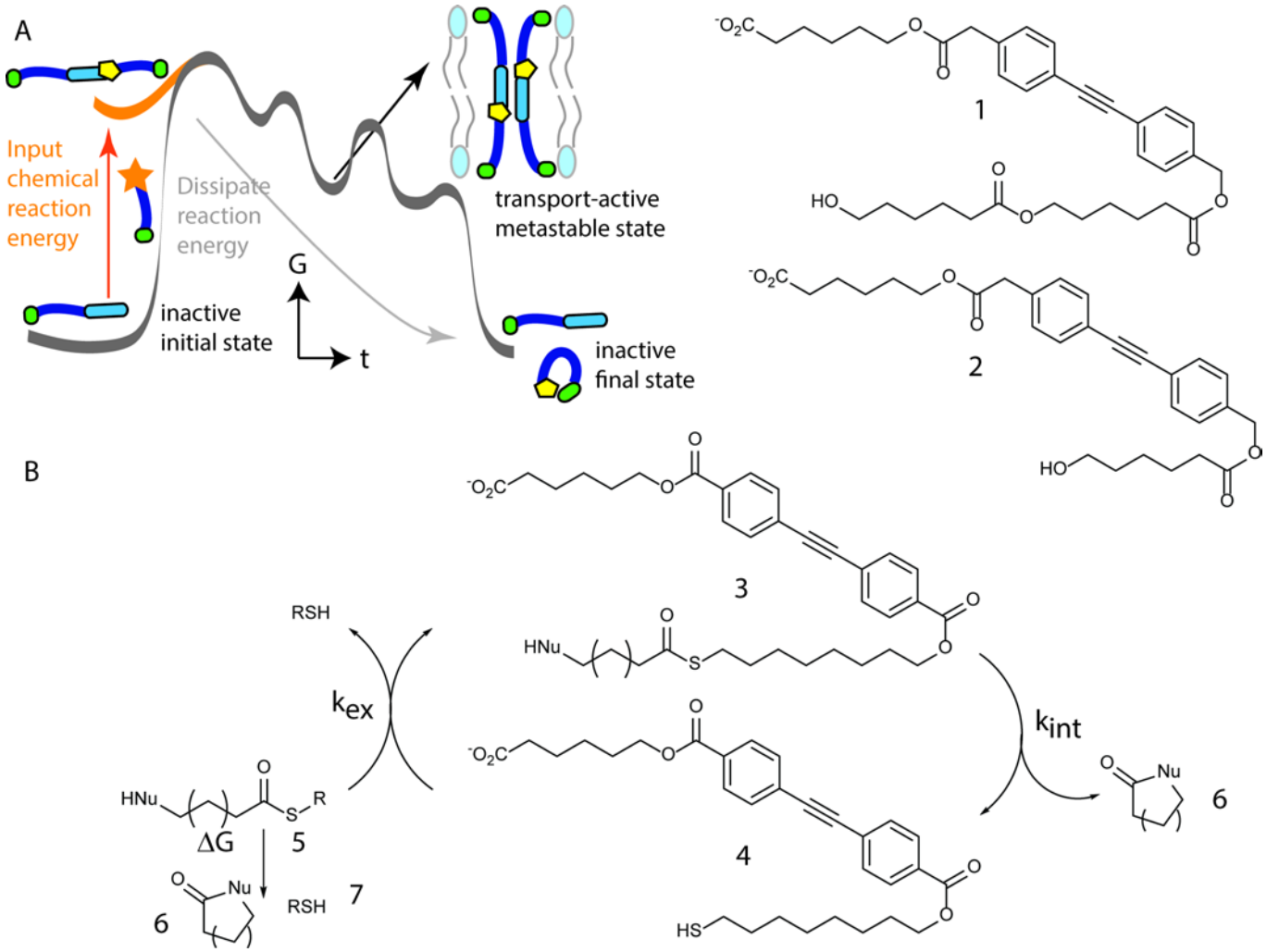

We report here the design and characterization of a system that shows dissipative assembly of a membrane transporter. From a design perspective, the system is required to function for transport only so long as a chemical source of energy is available. When the energy source is absent or exhausted, the system should not be capable of transport. It is important to note the distinction between the use of an energy source to create and maintain the transport system and the energy required as a driving force for the transport. We expect the system will always have available an externally applied driving force to energize ion translocation (e.g. an externally applied transmembrane potential), but will only function when an activating energy source is available that is capable of creating the transporter.

The conceptual design energetics are sketched in Figure 1A, where the energy transduction step to allow reaction free energy to initiate the assembly of a membrane-transport function would involve conversion of an inactive to an active transporter via a group transfer reaction. One possibility is that group transfer could remove a charge, for example a dephosphorylation that could shift an inactive charged compound to an active neutral. Another possibility is that the group transfer could alter the overall length and/or partition to shift between inactive and active states. The group transfer process is inherently bimolecular but the deactivation of the metastable state could be either uni- or bimolecular. More critical than the molecularity is the relative rate of the two processes; the rate of activation by group transfer must be significantly faster than any deactivation step so that the intermediate species will attain a sufficient concentration to induce the transport. A practical consideration is the rates of these processes relative to the experiments required to probe transport activity. Vesicle-based assays typically require ten minutes, so a convenient series of experiments to follow one activation/deactivation cycle would occupy a few hours[18]; a voltage-clamp experiment lies in the same time window[17]. Thus the group transfer should have a practical half-life of minutes and the deactivation process should have a practical half-life of less than an hour.

The general principles to create a membrane-spanning, hydrophilic pore are generally understood and there are many excellent examples as a point of departure for a dissipative assembly approach[19-29]. Less frequently reported are inactive structures related to compounds of high activity. The example which we chose to serve as the design lead structures are the previously reported oligoesters **1** and **2**[30, 31]. Compound **1** is highly active in both vesicle and voltage-clamp experiments while **2** has not shown any activity by voltage-clamp and is at least twenty-fold less active in vesicle experiments. The syntheses of this class of compounds relies on a limited set of optimized reactions and building blocks[30] so it is possible to anticipate making a library of compounds to optimize the required reaction kinetics.

In principle the group transfer reaction required could be effectively irreversible, but the rapid exchange reactions exploited in dynamic covalent assembly[32, 33], particularly a thiol-thioester exchange process[34], appeared to us to be simpler to incorporate into an overall system as the extent of a pseudo-equilibrium might be controlled with concentration. Thiol-thioester exchange is rapid for uncharged thiols[34] but is slower with thiols carrying anionic groups[35]; we expected an S for O substitution in the oligoester **1** to have only minor influence on transport activity. The thioester linkage then suggested that we focus on an intramolecular process to liberate a lactone (alcohol as nucleophile) or a lactam (amine as nucleophile). The rates of this intramolecular process are known to depend on the nature of the nucleophile and the tether length[36-38], providing structural control elements on the rate of deactivation. Thioester alcoholysis is the final stage in some polyketide macrocylizations and *in vitro* the rates are slow enough for long-chain derivatives to allow these species to be synthesized[39]. Ammonolysis reactions of thioesters lie at the heart of native chemical ligation and macrocyclization strategies[40, 41]; the ammonolysis rate is known to be slower than thiol-thioester exchange even for five-membered cyclic intramolecular intermediates. This rate must also be under the control of the medium pH which controls the effective concentration of the free amine nucleophile[38]. We did not explore a direct replacement of O by S in compounds **1** and **2** as a terminal thiol in place of the alcohol in **2** is potentially capable of a second intramolecular thiolysis of the next O-ester down the chain. We opted to slow this potentially competing process by extending the carbon chain and reversing the orientation of the ester to generate candidate structures **3** and **4** (Fig. 1B). The chemical fuel required for this system is therefore **5** and the free energy of the dissipative assembly is provided via intramolecular cyclization to the lactone or lactam **6** plus a thiol (**7**). Although we did not have detailed kinetic information at this design stage, the suite of compounds and the potential for pH and concentration control of the rates should provide enough scope for experimental exploration.

Synthesis: The synthesis (Scheme 1) utilized previously developed protocols for most of the required steps[30, 31]. Starting with the prenyl ester protected 6-hydroxyhexanoate (**8**), standard ester coupling with 4-iodobenzoic acid afforded **9** which underwent Sonogashira coupling with trimethylsilylacetylene using an established protocol[30]. The silyl group of **10** was cleaved with fluoride to give the terminal alkyne **11** in 70% yield over the three steps. The nucleophilic end of the targets was prepared from Boc-protected ω-aminoalkanoic acids (**12a-d**) or protected ω- hydroxyalkanoic acids (**13e,f**) coupled under standard conditions with stoichiometric 8-mercapto-1-octanol (**14**). Thioesters **15a-f** were isolated in yields of 35-50% from the mixture of unreacted **14**, and minor O-ester components.

Scheme 1: Synthesis of required components

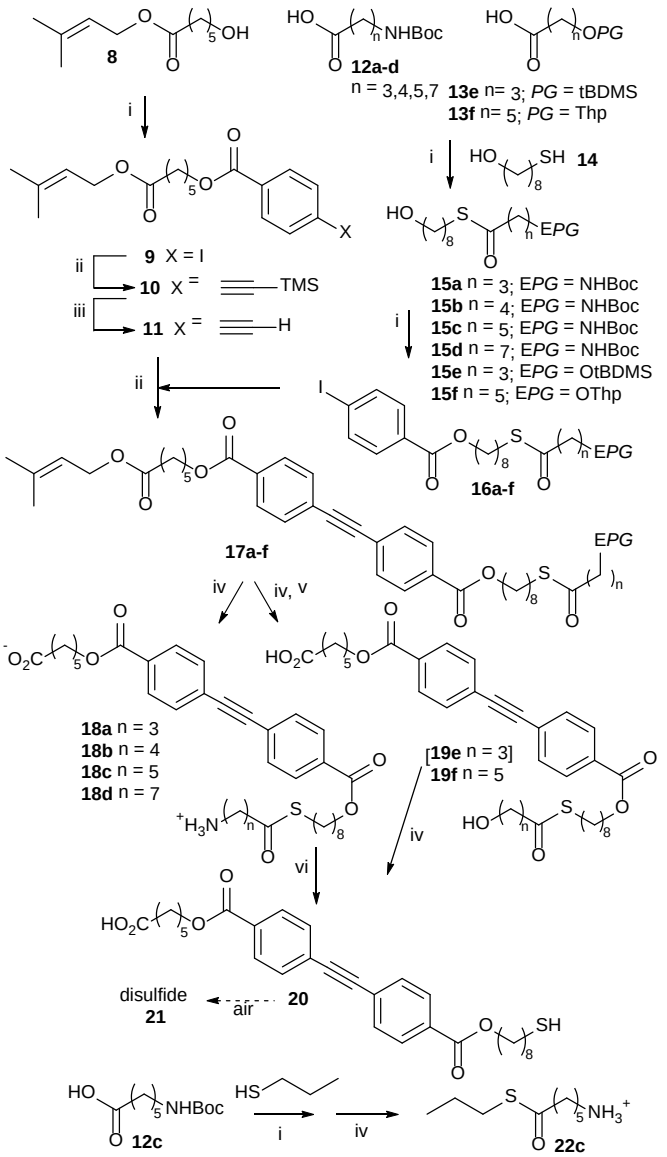

Conditions: i) THF, DIC, HOBt, DIPEA, RT, 16h, 83-99%; ii) DMF, 0.03 eq. $Pd(PPh_3)_4$, 0.06 eq. CuI, 2.4 eq. Et_3N, 59-95%; iii) a) THF, 1 eq. TBAF, RT, 10 min, b)excess MeOH 63-83%; iv) DCM, 1.25 eq. TMSOTf, 0°C to RT, 4 h, precipitate in hexanes 40-80%; v) DCM-MeOH (9:1), 0.2 eq TsOH, RT, 3h, 24%; vi) a) $CHCl_3$, 10 eq. $NaHCO_3$(aq), 40°C, 4h, b) 0°C, HCl to pH 2.

Standard Sonogashira coupling[30] of alkyne **11** with the iodides **16a-f** gave protected targets **17a-f** in acceptable to excellent yields. Concurrent cleavage of Boc and prenyl protecting groups was achieved with trimethylsilyl triflate[30]; the cleavage conversion was high in all cases, but the isolation by precipitation of the zwiterionic product in hexanes gave variable yields of isolated **18a-d**. Concurrent cleavage of the prenyl and *t*-butyldimethylsilyl protecting groups[30] of **17e** failed to produce the expected **19e**, giving instead the degraded

thiol **20** in modest yield. This disappointing result at least establishes that the required deactivation step of Fig 1b is possible. Stepwise removal of the prenyl and tetrahydropyranyl groups of **18f** gave **19f** as an isolable material albeit with significant loss in the Thp cleavage step. All final compounds were additionally purified by semi-preparative HPLC to ensure high purity samples were used in the subsequent work.

The thiol **20** can be prepared from **18a-d** in a two-phase system of chloroform and aqueous bicarbonate which results in good conversion but suffers losses on workup. Samples can be characterized as the thiol, but air oxidation to the disulphide (**21**) occurs readily (Electronic Supplementary Information†) and this material is best prepared and handled under inert atmosphere. Finally, the required chemical fuel (e.g. **22c**) can be prepared from **12c** and propane thiol using standard conditions; **22c** is unstable to basic conditions and is handled as the salt. Full synthetic details are given in the Electronic Supplementary Information (ESI)†.

Solution reactions: We first need to establish if the expected reactions occur at reasonable rates and to settle on a suitable compound for transport evaluation. We were initially interested in the kinetics under the dilute conditions suited to membrane transport experiments so we conducted a survey of the stability of compounds **18a-d** and **19f** in 1% water in acetonitrile with added base (di-isopropyl ethyl amine) using HPLC to monitor the disappearance of the starting compound. Quantitative experiments utilized an internal standard (triethyleneglycol methylether diester of 4,4'-diphenylacetylene dicarboxylate) containing the same chromo- and fluorophore. The alcohol **19f** appeared to be stable under these conditions, but the amines decomposed as expected, albeit at modest rates due to the low solvent polarity[34](Fig S-1 ESI†).

The thioester exchange reactions proved to be difficult to monitor by HPLC due to the limited solubility of **22c** in solvents compatible with the HPLC experiment. We therefore explored the relative rates of thioester exchange and intramolecular decomposition using NMR (DMSO: D_2O 3:1; 2 eq. NaOD). For spectral simplification we used benzyl thiol in place of **20**. The required thioester exchange reaction occurs very rapidly relative to the intramolecular decomposition which produces the expected valerolactam (Figs S-2, S-3 ESI†). Again, the intramolecular process appears to be relatively slow under the NMR concentration conditions, but the underlying reactions and relative rates required for the design appear to in place.

Transport: The next task is to establish the transport activity of the compounds prepared, and the inactivity of the thiol **20**. We were very disappointed to discover that compounds **18a-d** and **19f** are quite inactive in a vesicle-based transport assay using HPTS (Fig S-4 ESI†). This is not due to competing aqueous aggregation[30, 31] as there is significant partition to vesicles of compounds **18a** and **18d** as assessed by solvent-dependent steady-state fluorescence (Fig S-5 ESI†).

Transport activity can be detected in planar bilayers by the voltage-clamp experiment[17] (Figure 2). The alcohol-terminated compound **19f**, expected to be stable based on solution studies, produced multi-level and erratic activities that are directly comparable to the activity previously found for **1** (Fig.2A). The comparison of these irregular activities relies heavily on the previously described activity-grid methodology which displays the duration and conductance of transport events on a log-log grid with colours to indicate the types of activities observed. The compounds of Fig. 2 showed only short duration spikes (red), multi-level discrete openings (Fig 2A top trace; blue) and erratic (Fig. 2A lower trace, purple). In the summary grids provided, the relative frequency of a particular activity is indicated by colour density. It is the overall pattern that allows comparison, rather than any individual feature of the raw data.

Figure 2: Voltage-clamp activity of individual compounds[a]: A, **19f**; B, **18c**; C, **21** produced from **20** in air; D, **20** under Ar.

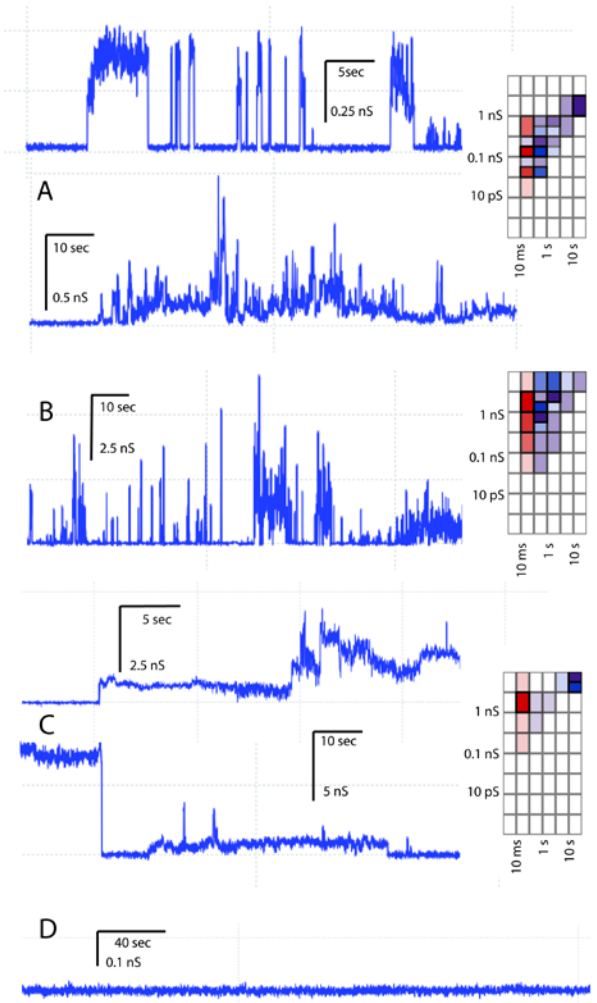

a) A-C: diPhyPC, 1M CsCl, 10 mM HEPES + 10mM Tris buffer pH 7.0 in air for A-C; D: diPhyPC, 1M CsCl, 10 mM Tris/TrisHCl pH 8.3 under Ar atmosphere with Ar sparged solutions.

The amines **18a-d are** less active than the alcohol **19f** in the sense that transport activity is more difficult to initiate; **18c** is the most reliably active. Once channels are observed, they produced generally shorter open durations than **19f** as indicated by the shift in the colour density to the left in the grid of Fig 2B. Since we require reliable activity for the dissipative assembly experiments, we focussed on 18c and explored a number of voltage-time procedures in an attempt to reliably stimulate activity. Compound **18c** has a voltage-dependent conductance profile. Between -80 and 80 mV applied potential

the channels are Ohmic with a specific conductance of 85 ± 35 pS, but increasing positive or negative potential outside this range results in a steady increase in conductance rising to ~ 1.5 nS at ±150 mV. This type of behavior has been sought but not previously observed for this type of oligoester channel[17]. Similar non-linear conductance changes do occur in aromatic-core oligoester channels terminated in amines[42, 43]. A mechanistic analysis is deferred, but the practical implications are important for the dissipative assembly experiment. Firstly the appearance of the activity grid will be voltage-dependent. Note the increase in the conductance of **18c** relative to **19f** evident in the grids of Figs. 2A and 2B; this reflects the generally higher potential required for strong channel activity of **18c**. This is a complicating factor, which is offset by the observation that reliable activity can be induced for **18c** via a short period of applied potential in excess of ±130 mV. The applied potential may be reduced after this "kick". It will thus be able to probe for the presence of **18c** in a bilayer which appears to be generally inactive. Subsequent experiments with **18c** will use pH 8.2-8.4 compared to pH 7.0 of Fig. 2B but we will compare the activity grids directly. We cannot detect a clear difference between the two conditions based on the experimental summaries given in the Electronic Supplementary Information†.

Initial experiments with compound **20** were profoundly puzzling and disappointing; this is the most active synthetic ion channel we have handled in two decades. As shown in Fig. 2C, the activity of **20** in air-saturated solution is almost exclusively long-duration (>100 seconds) high conductance (>3 nS) erratic activity. Fig. 2C shows that these channels initiate via lower conductance periods but terminate in an abrupt transition to the baseline. Onset of channel activity is quick, and once establish appears to continue indefinitely. This activity is completely unexpected based on the very low activity of **2** and it took some time to recognize that even small amounts of oxidation of **20** to the disulphide **21** could produce enough of the latter compound to give the activity detected. Fig. 2D shows the typical "activity" of an Ar purged system containing **20**. Again we defer a mechanistic analysis of the channel formed by **21**, but in this case the possible presence of **21** as a contaminant requires additional controls in the projected dissipative assembly experiments. Specifically, we will need to show that any activity that appears later in an experiment is *not* a result of accidental oxidation during prior manipulations. A purple long-lived, high conductance cell in the upper-right of the activity grid will be a clear indicator of such contamination.

Experimental protocols for reaction monitoring using membrane activity: With the individual components characterized, we next require a protocol to monitor transport activity as the system evolves via chemical reactions. We begin this stage with experiments to show that the inactivity of traces like Fig. 2D, which we assert contain the thiol **20** in the bilayer, can be converted to activity similar to Fig. 2C through the introduction of a small amount of air. Such an experiment is shown in Figure 3. Direct real-time inspection of the current–time profile is very difficult. The compounds show erratic activity as their normal behaviour and all current traces of such activity look the same. We also need to vary the applied potential in response to conditions in the experiment. To address this, we settled on a procedure where the current-time and voltage-time profiles are displayed (Fig. 3A, 3B) in conjunction with an averaged conductance for defined intervals (5 min. in Fig. 3C). The latter display is coarse-grained but pulls the essential information from highly fluctuating signals. The injection of two 10μL bubbles of air at the point marked rapidly produces both an obvious current response as well as a jump in the conductance trace (Fig. 3C). The activity grid for the activity following the air injection is strongly similar to the activity grid for **21** (Fig. 2C), especially in the dominant high conductance, long duration region. We conclude that this experiment establishes the potential of such experiments to detect the activity from, and the identity of, a very small amount of a functional transporter.

Figure 3: Reaction monitoring by voltage-clamp for the air oxidation of thiol **20**[a]

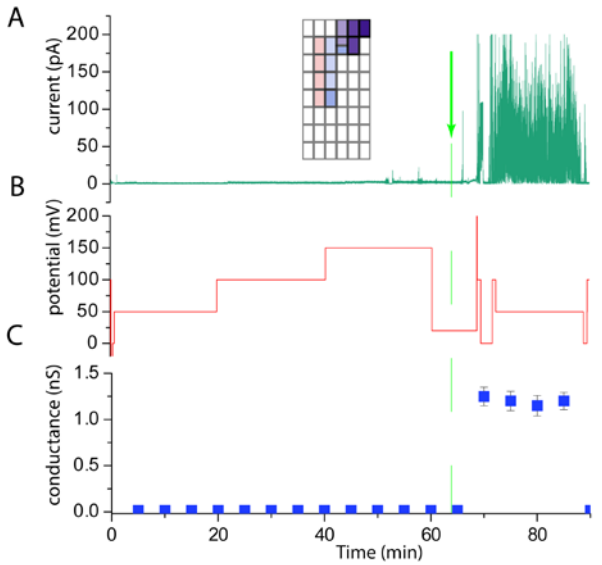

a) diPhyPC, 1MCsCl, 10 mM Tris/Tris HCl, pH 8.25, Ar atmosphere and Ar sparged solutions). A: current-time profile; B: applied potential as a function of experiment time; C: average conductance (5-minute interval) as a function of experiment time. At the time indicated by the green arrow, two 10 μL bubbles of air were injected near the bilayer. The inset grid applies to 10 minutes of data between 75 and 85 min.

An essential reaction is the expected decline in activity of **18c** as it reacts to produce **20**. Figure 4A shows current-time and average conductance-time profiles for an experiment containing **18c** at pH 8.3 (the voltage-time profile is omitted for simplicity; it was +125 to +150 mV for most of the experiment). The die-off in activity is evident, but appears to occur more quickly than in the solution studies. This reflects the higher-order nature of channel formation in which the activity declines as some power of the concentration of **18c**. Note as well that the erratic nature of the channels formed by **18c** make quiescent periods within the "active" part of the profile; the conductance-time profile averages the irregularities at the expense of time resolution.

We can establish that **20** is produced using the previous experiment, but we also can suppress the die-off by providing a large excess of **22c** that is expected to react with **20** to maintain the concentration of **18c**. This experiment is illustrated in Figure 4B over a span that is three-fold longer than the experiment of Fig. 4A. Compound **22c** alone is inactive for transport (early section of Fig. 4B and ESI†) but the activity from **18c** is initiated rapidly once added and is sustained in the presence of **22c**. The inset activity grid for the last hour of this experiment is similar to that of Fig. 2B for **18c**. Had any

accidental oxidation occurred we would expect to see the long-lived high conductance erratic activity of **21**. This activity is absent in the trace, although the potential for accidental oxidation is low from the way this experiment was conducted.

Figure 4: Transport activity of **18c** in the absence (A) and presence (B) of the fuel **22c**[a].

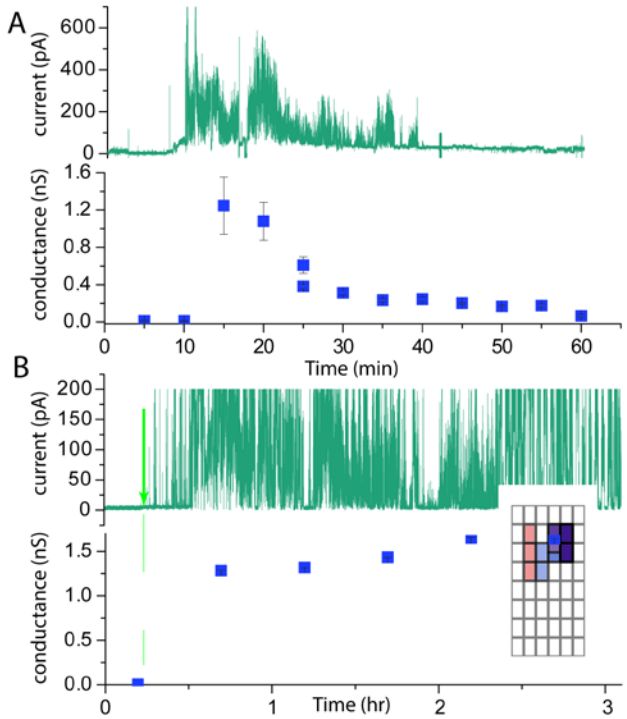

a) diPhyPC, 1M CsCl, 10mM Tris/TrisHCl, pH 8.3, Ar atmosphere and Ar sparged solutions Both experiments contained 90 nmol **18c** (injected at t=0 in A and at the arrow in B). **22c** initial conc. was 1.4 mM

Dissipative assembly: With the foregoing controls and protocols in place, we finally turn to experiments in which dissipative assembly might be detected. Two such experiments are given in Figure 5. Both start with **18c** in the bilayer system. In Fig 5A-C) the compound was added to a pre-formed bilayer just prior to the period illustrated. Activity was established and over the first hour gradually subsided. The voltage-time record (Fig. 5B) shows high potentials throughout the period, so the decrease in the average conductance trace (Fig. 5C) prior to 60 minutes is good evidence that the concentration **18c** has decreased. The arrow indicates the point at which **22c** was added, dissolved in a small amount of buffer. Early experiments had established that stirring was not possible, so the plug of solution was inserted and spread solely by diffusion. Following a delay of about 10 minutes, clear activity is generated and this falls off near the end of the period illustrated. The inset activity grid is derived for 15 minutes of activity after the injection; it is similar to Fig. 2A and quite distinct from Fig. 2C or Fig. 3. We conclude that the activity generated is due to regenerated **18c** as required in the design and not due to accidental oxidation of **20**.

If we wish to see multiple cycles within a reasonable lifetime of a bilayer, then we need much less **18c** invested in the experiment so that a pulse of **22c** will create a local concentration of **18c** high enough to initiate channels, but low enough so that the decomposition and diffusion processes rapidly reduce this local concentration to a point where channel formation is unfavourable. Fig. 5 D-F shows an example in which the transporter was blended in the lipid prior to bilayer formation to result in a system with about 750-fold less **18c** invested. The overall activity level is low and further truncated by the long duration of the Figure. The initial die-off of activity is clear in the conductance-time record. Addition of **22c**, again unstirred, at the indicated points results in short pulses of activity delayed by 5-10 minutes from the times of addition. At higher time resolution these consist of periods of erratic activity over 2-10 minutes. The inset activity grid for the late activity is consistent with **18c** not **20**. The pulses are not uniform in duration, likely due to inhomogeneity in the dispersion of the injected plug of **22c** and the follow-on effect on the concentration of **18c** produced.

Conclusions

We believe the foregoing constitutes experimental demonstration of the dissipative assembly of a functional transport system. The design contained the following elements that we have been able to demonstrate experimentally: i) intermolecular thioester exchange occurs rapidly from **22c** as required in the group transfer approach of the design; ii) intramolecular degradation of **18c** with release of a lactam occurs more slowly to give the required relative rates of the competing kinetic processes; (in the absence of air); iii) the designed active (**18c)** and inactive transporters (**20**) perform correctly, albeit with predominantly erratic activity; iv) the activity of the active species **18c** degrades in time, but can be significantly prolonged in the presence of excess **22c** fuel; and v) the system can cycle from inactive to active and back via injection of **22c** as a fuel.

The foregoing also highlights some weaknesses in the design, not the least of which is the unusually high activity of the disulphide **21**. This species is so easily formed and detected that it can completely mask the designed function. The very high sensitivity of the system to small amounts of air does however indirectly point to why the state of the system can be so readily manipulated with external reagents. Both the oxidation of **20** to **21** and the thioester exchange reaction of **22c** with **20** to produce **18c** are bimolecular processes. Both reactive partners are in low bulk concentration so rates would be expected to be low. The relatively fast system response rate in both cases must arise via reactions in which the reactive partners have a higher relative concentration through association with the bilayer membrane. We note that the *bulk* concentration of **22c** at the end of the experiment illustrated in Fig. 5 D-F is four-fold higher than the *bulk* concentration in Fig. 4B. The obvious differences in system activity between these two experiments are therefore due inhomogeneity in the distribution of **22c** controlled by diffusion in the unstirred experiment of Fig. 5. We do not know what the true concentrations of the reactive partners might be so we do not know how fast the channel-forming species **21** or **18c** are formed. But it follows that whenever they form, they do so within the bilayer so are immediately available to seek partners for assembly to active channels. Channel-formation is potentially another high kinetic-order process and the relatively brief pulses of activity in Fig. 5 D-F suggest that diffusion within the bilayer also limits local concentrations of channel-forming monomers. At every time in every experiment there is

Figure 5: Dissipative assembly of a membrane transport system based on **18c** initially present with fuel **22c** added at the arrows[a].

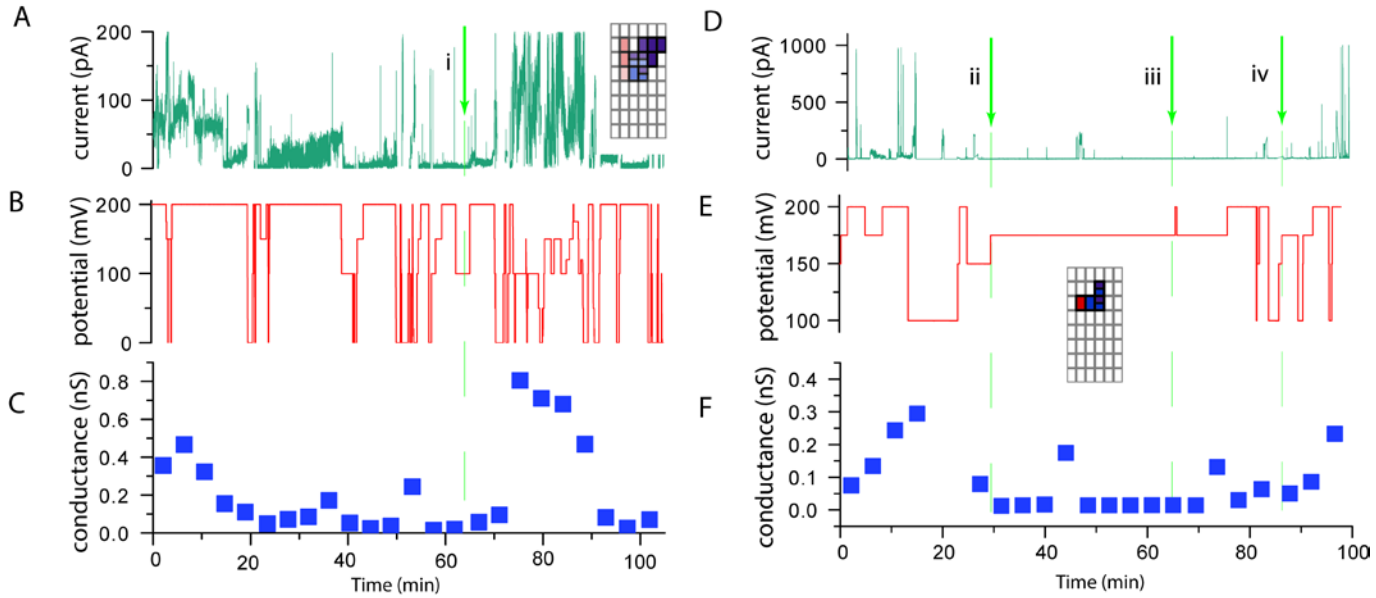

a) diPhyPC, 1MCsCl, 10 mM Tris/Tris HCl, pH 8.3, Ar atmosphere, Ar sparged solutions. A-C) 74 nmol **18c** added in MeCN 12 minutes prior to t=0; 22µmol **22c** in 100µL buffer added at i without stirring. D-F) **18c** 0.18 mol% in lipid, approx. 0.1 nmol in cell; 22 µmol, 26 µmol, and 36µmol **22c** added at ii, iii, and iv without stirring.

a vast excess of the components required to form detectible channels. That the system appears inactive much of the time in most experiments simply reflects kinetic barriers and spatial inhomogeneity. Our external control of the system does include a control of chemical potential (concentration), but dissipative assembly is, at its heart, a kinetic phenomenon. This system demonstrates that fact of life.

Acknowledgement

The sustaining support of the Natural Sciences and Engineering Research Council of Canada and the University of Victoria is gratefully acknowledged.

Notes and references

[a] Department of Chemistry, University of Victoria, PO Box 3065, Victoria, BC, Canada V8W 3P6; tel: (250 721 7192; fax (250) 721 7147; e-mail: tmf@uvic.ca.

† Electronic Supplementary Information (ESI) available: synthetic procedures for all compound, solution kinetic experiments, transport activity in vesicles, and voltage clamp procedures. Additional summary activity records of compounds **19f**, **18c**, and **21** are available at: http://hdl.handle.net/1828/5270.

1. M. Boden, *The British Journal for the Philosophy of Science*, 1999, **50**, 231-248.
2. F. Capra, *Theory, Culture & Society*, 2005, **22**, 33-44.
3. M. Fialkowski, K. J. M. Bishop, R. Klajn, K. Smoukov, C. J. Campbell and B. Grzybowski, *J. Phys. Chem. B.*, 2006, **110**.
4. J. R. Green, A. B. Costa, B. A. Grzybowski and I. Szleifer, *Proceedings of the National Academy of Sciences*, 2013, **110**, 16339-16343.
5. G. M. Whitesides and B. Grzybowski, *Science*, 2002, **295**, 2418-2421.
6. B. Grzybowski, C. E. Wilmer, J. Kim, K. P. Browne and K. J. M. Bishop, *Soft Matter*, 2009, **5**, 1110-1128.
7. A. N. Zaikin and A. M. Zhabotinsky, *Nature*, 1970, **225**, 535-537.
8. Q. Ouyang and H. L. Swinney, *Nature*, 1991, **352**, 610-612.
9. T. J. Bansagi, V. K. Vanag and I. R. Epstein, *Science*, 2011, **331**, 1309-1312.
10. B. A. Grzybowski, H. A. Stone and G. M. Whitesides, *Nature*, 2000, **405**, 1033-1036.
11. J. V. I. Timonen, M. Latikka, L. Leibler, R. H. A. Ras and O. Ikkala, *Science*, 2013, **341**, 253-257.
12. A. Desai and T. J. Mitchison, *Annual Review of Cell and Developmental Biology*, 1997, **13**, 83-117.
13. H. Hess, J. Clemmens, C. Brunner, R. Doot, S. Luna, K.-H. Ernst and V. Vogel, *Nano Letters*, 2005, **5**, 629-633.
14. H. Liu, E. D. Spoerke, M. Bachand, S. J. Koch, B. C. Bunker and G. D. Bachand, *Advanced Materials*, 2008, **20**, 4476-4481.
15. C. Z. Dinu, J. Opitz, W. Pompe, J. Howard, M. Mertig and S. Diez, *Small*, 2006, **2**, 1090-1098.
16. J. Boekhoven, A. M. Brizard, K. N. K. Kowlgi, G. J. M. Koper, R. Eelkema and J. H. van Esch, *Angew. Chem. Int. Ed. Eng.*, 2010, **49**, 4825 –4828.
17. J. K. W. Chui and T. M. Fyles, *Chem. Soc. Rev.*, 2012, **41**, 148-175.
18. S. Matile and N. Sakai, in *Analytical Methods in Supramolecular Chemistry*, ed. C. A. Schalley, Wiley -VCH, Weinheim, 2007, pp. 381-418.
19. Y. Zhao, H. K. Cho, L. Widanapathirana and S. Y. Zhang, *Accounts Chem. Res.*, 2013, **46**, 2763-2772.
20. P. Reiss and U. Koert, *Accounts Chem. Res.*, 2013, **46**, 2773-2780.

21. J. Montenegro, M. R. Ghadiri and J. R. Granja, *Accounts Chem. Res.*, 2013, **46**, 2955-2965.
22. Y. Kim, W. Li, S. Shin and M. Lee, *Accounts Chem. Res.*, 2013, **46**, 2888-2897.
23. A. V. Jentzsch, A. Hennig, J. Mareda and S. Matile, *Accounts Chem. Res.*, 2013, **46**, 2791-2800.
24. G. W. Gokel and S. Negin, *Accounts Chem. Res.*, 2013, **46**, 2824-2833.
25. T. M. Fyles, *Accounts Chem. Res.*, 2013, **46**, 2847-2855.
26. F. De Riccardis, I. Izzo, D. Montesarchio and P. Tecilla, *Accounts Chem. Res.*, 2013, **46**, 2781-2790.
27. G. W. Gokel and S. Negin, *Advanced Drug Delivery Reviews*, 2012, **64**, 784-796.
28. S. Matile, A. V. Jentzsch, J. Montenegro and A. Fin, *Chemical Society Reviews*, 2011, **40**, 2453-2474.
29. T. M. Fyles, *Chem. Soc. Rev.*, 2007, **36**, 335-347.
30. J. Moszynski and T. M. Fyles *J. Am. Chem. Soc.*, 2012, **134**, 15937−15945.
31. J. M. Moszynski and T. M. Fyles, *Org. Biomol. Chem.*, 2010, **8**, 5139-5149.
32. Y. Cheng, H. Peng and B. Wang, in *Supramolecular Chemistry*, John Wiley & Sons, Ltd, 2012.
33. K. Meguellati and S. Ladame, in *Constitutional Dynamic Chemistry*, ed. M. Barboiu, Springer Berlin Heidelberg, 2012, vol. 322, ch. 277, pp. 291-314.
34. P. J. Bracher, P. W. Snyder, B. R. Bohall and G. M. Whitesides, *Origins of life and evolution of the biosphere : the journal of the International Society for the Study of the Origin of Life*, 2011, **41**, 399-412.
35. F. M. Mansfield, Y. A.-Y. Ho, J. K. M. Sanders and S. Otto, *J. Syst. Chem.*, 2010, **1**, 12-25.
36. C. Galli, G. Illuminati, L. Mandolini and P. Tamborra, *Journal of the American Chemical Society*, 1977, **99**, 2591-2597.
37. C. Galli and L. Mandolini, *Eur. J. Org. Chem.*, 2000, 3117-3125.
38. D. F. DeTar and N. P. Luthra, *Journal of the American Chemical Society*, 1980, **102**, 4505-4512.
39. N. M. Gaudelli and C. A. Townsend, *The Journal of Organic Chemistry*, 2013, **78**, 6412-6426.
40. C. J. White and A. K. Yudin, *Nat Chem*, 2011, **3**, 509-524.
41. L. Zhang and J. P. Tam, *Journal of the American Chemical Society*, 1997, **119**, 2363-2370.
42. Y. Zong, M.Sc., University of Victoria, 2014.
43. J. K. W. Chui, T. M. Fyles and H. Luong, *Beilstein J. Org. Chem.*, 2011, **7**, 1562-1569.

